Plant regrowth as a driver of recent enhancement of terrestrial CO_2 uptake

Running Title: CO_2 uptake by plant regrowth

Masayuki Kondo[1], Kazuhito Ichii[1,2], Prabir K. Patra[3], Benjamin Poulter[4], Leonardo Calle[5], Charles Koven[6], Thomas A. M. Pugh[7,8], Etsushi Kato[9], Anna Harper[10], Sönke Zaehle[11], Andy Wiltshire[12]

[1]Center for Environmental Remote Sensing (CEReS), Chiba University, Chiba, Japan.

[2]Center for Global Environmental Research, National Institute for Environmental Studies, Tsukuba, Japan.

[3]Research and Development Center for Global Change, Institute of Arctic Climate and Environment Research/ Project Team for Advanced Climate Modeling, Department of Environmental Geochemical Cycle Research, Japan Agency for Marine-Earth Science and Technology, Yokohama, Japan.

[4]NASA Goddard Space Flight Center, Biospheric Science Laboratory, Greenbelt, Maryland 20771, USA.

[5]Institute on Ecosystems and Department of Ecology, Montana State University, Bozeman, Montana 59717, USA.

[6]Earth Sciences Division, Lawrence Berkeley National Laboratory, Berkeley, CA 94720, USA.

[7]Institute of Meteorology and Climate Research, Environmental Atmospheric Research (IMK-IFU), Karlsruhe Institute of Technology (KIT), Kreuzeckbahnstraße 19, 82467 Garmisch-Partenkirchen, Germany

[8]School of Geography, Earth & Environmental Science and Birmingham Institute of Forest Research, University of Birmingham, B15 2TT, UK

[9]Institute of Applied Energy, Tokyo, 105-0003, Japan.

[10]University of Exeter, Exeter EX4 4QF, UK.

[11]Biogeochemical Integration Department, Max Planck Institute for Biogeochemistry, 07701 Jena, Germany.

[12]Met Office Hadley Centre, Fitzroy Road, Exeter EX1 3PB, UK.

Corresponding Author:

Masayuki Kondo

Center for Environmental Remote Sensing (CEReS), Chiba University

1-33 Yayoi-cho Inage-ku, Chiba, 263-8622, Japan

Tel/Fax: +81-43-290-3860

E-mail: redmk92@gmail.com

Key Points

Main point #1: The recent enhancement of CO_2 uptake by the land cannot be explained without a contribution from plant regrowth from past land use changes.

Main point #2: Ecosystems induce a strong tendency toward a net sink for the past 50 years when the effect of land use changes is taken into account.

Main point #3: North America, Europe, and temperate Eurasia account for 94% of the global total CO_2 uptake enhancement by plant regrowth.

Abstract

The increasing strength of land CO_2 uptake in the 2000s has been attributed to a stimulating effect of rising atmospheric CO_2 on photosynthesis (CO_2 fertilization). Using terrestrial biosphere models, we show that enhanced CO_2 uptake is induced not only by CO_2 fertilization, but also an increasing uptake by plant regrowth (accounting for 0.33±0.10 Pg C yr^{-1} increase of CO_2 uptake in the 2000s compared with the 1960s−1990s) with its effect most pronounced in eastern North America, southern-eastern Europe, and southeastern temperate Eurasia. Our analysis indicates that ecosystems in North America and Europe have established the current productive state through regrowth since the 1960s, and those in temperate Eurasia are still in a stage from regrowth following active afforestation in the 1980s−1990s. As the strength of model representation of CO_2 fertilization is still in debate, plant regrowth might have a greater potential to sequester carbon than indicated by this study.

Keywords: carbon budget, plant regrowth, CO_2 fertilization, land use change, biosphere model

1. Introduction

CO_2 accumulates in the atmosphere as a result of greater anthropogenic emissions due to fossil fuel consumption and cement production compared to the net uptake by the land and ocean (Le Quéré et al., 2016). Although atmospheric CO_2 has been consistently increasing from the industrial era, the airborne fraction has declined from the early 2000s because of an enhancement in CO_2 uptake by the land and ocean (Keenan et al., 2016; Sarmiento et al., 2010), which has doubled during the past 50 years and is predicted to remain strong hereafter (Ballantyne et al., 2012). Mechanisms behind the enhanced CO_2 uptake involve physiological and biogeochemical processes on both the land and ocean (Ballantyne et al., 2017; DeVries et al., 2017; Keeling et al., 2017; Keenan et al., 2016; Sarmiento et al., 2010), but the land is of primary importance because it has a larger control on the interannual growth rate of atmospheric CO_2 (Cox et al., 2013; Wang et al., 2013), and is thus believed to be more responsible for the recent slowing down of surface warming (Fyfe et al., 2016; Shevliakova et al., 2013).

Growing evidence suggests that the enhancement of CO_2 uptake by the land is primarily due to the effect of CO_2 fertilization (Fisher et al., 2013; Keenan et al., 2016; Sun et al., 2014), which has led to a greening of a large fraction of the terrestrial biosphere (Zhu et al., 2016) and compensated for large CO_2 emissions resulting from tropical land use (Schimel et al., 2015). An experiment with an Earth system model suggests that the observed rise of ~115 ppm in atmospheric CO_2 since the preindustrial era might have been higher by ~85 ppm without the effect of CO_2 fertilization (Shevliakova et al., 2013), implying a large contribution of CO_2 fertilization to net CO_2 flux (balance between CO_2 uptake and release by the terrestrial biosphere). However, it is still arguable whether the CO_2 fertilization is a dominant cause for the recent enhancement of CO_2 uptake because, in addition to the level of atmospheric CO_2, the terrestrial biosphere has undergone historical changes through land use and management (Erb et al., 2013, 2018). CO_2 emissions resulting from land use change (LUC) activities account for ~9% of the total global anthropogenic CO_2 emissions (Le Quéré et al., 2016), therefore changes in LUC could affect the course of the net sink-source pattern of CO_2 over time. The recent declining trend in global LUC activities (Houghton & Nassikas, 2017) implies likely reductions in CO_2 release from land use and land cover change (LUC emissions, hereafter) and increases in uptake by plants recovering from past LUC (regrowth flux, hereafter). Pacala et al. (2001) demonstrated that forest regrowth in the eastern US accounted for much of the land uptake in the region during the 1980s, thus identifying regrowth as a potentially globally significant flux. However, quantification of such changes over the recent period has not been fully addressed before and contribution of LUC fluxes to the recent terrestrial CO_2 uptake is not clearly understood. Neglecting contributions from LUC fluxes would lead to incomplete understanding of processes involved in the climate-carbon cycle feedback and future pathways to climate change mitigation.

For a better understanding of mechanisms behind the recent enhancement of land CO_2 uptake, we investigate global and regional patterns of relative contributions to net CO_2 uptake through an attribution study using an ensemble of biosphere models from TRENDY, in conjunction with independent net CO_2 flux estimates that are estimated to be optimally consistent with atmospheric CO_2 measurements (atmospheric CO_2 inversion) and CO_2 growth rate (a residual land uptake from Global Carbon Project: GCP). Through the evaluation of the relative contributions (i.e., CO_2 fertilization effect, climate effect, LUC emissions, and regrowth flux) to the past and current CO_2 uptake, we address the role of historical LUC in the recent uptake enhancement.

2. Methods

2.1. Sign convention for net CO_2 flux

In this analysis, we chose the sign convention for net CO_2 flux that is commonly used in top-down analyses: the negative sign (–) for a net sink to the land and the positive sign (+) for a net source to the atmosphere. This sign convention is used for all components of this study and thus applied to terms for CO_2 exchange such as Net Biome Production (NBP) and Net Ecosystem Production (NEP). It should be noted that this convention is opposite to the one commonly used in bottom-up analyses (Chapin et al., 2006).

2.2. Terrestrial biosphere models

2.2.1. TRENDY models

Simulations of the biosphere models used in this study are from the TRENDY v2 (Sitch et al., 2015; Zhao et al., 2016). The TRENDY models were run with a consistent forcing dataset: (1) atmospheric CO_2 mixing ratio for 1860−2012 based on ice-core measurements and station observations, (2) climate dataset for 1901−2012 based on a merging between Climate Research Unit (CRU) TS3.2 0.5° × 0.5° monthly climate data (Harris et al., 2014) and National Centers for Environmental Prediction (NCEP) and National Center for Atmospheric Research (NCAR) Reanalysis 2.5° × 2.5° 6-hourly climate data (Kistler et al., 2001), and (3) 0.5° × 0.5° gridded annual LUC dataset for 1860−2012. The TRENDY models were run following a common protocol: simulation that considers variability in atmospheric CO_2 only (S1); simulation that considers variability in CO_2 and climate (S2); and simulation that considers variability in CO_2, climate, and historical LUC (S3). For each simulation, the models were first spun-up to an equilibrium state of carbon balance forced with the 1860 CO_2 mixing ratio (287.14 ppm), recycling climate mean and variability from the early decades of the 20th century (i.e., 1901−1920), and using constant 1860 crop and pasture distribution. S1, S2, and S3 simulations were then conducted for a transient period 1861−2012 after initialization from these spin-up runs.

2.2.2. Attributions to net CO_2 flux

Attributions to net CO_2 flux were extracted by separating flux signals in the simulations S1, S2, and S3 (Table 1). NBP of the S3 (forced with varying CO_2, climate, and LUC) represents a best estimate of the actual net CO_2 flux of the terrestrial biosphere. NBP from the S1 and S2 simulations represent partial contributions to net CO_2 flux, representing the CO_2 (fertilization) effect and CO_2 +climate effects on net CO_2 flux, respectively. The climate effect was extracted by subtracting NBP of the S1 from that of the S2; their difference leaves out the effect of CO_2 fertilization, and only the effect of climate remains (Table 1).

Net LUC flux (a partial contribution to net CO_2 flux associated with LUC) was extracted by subtracting NBP of the S2 from that of the S3; their difference leaves out the effects of CO_2 fertilization and climate, and only the effect of LUC remains (to be precise, residuals of the CO_2 and climate effects remain due to changing land cover types). Further, we decomposed net LUC flux into regrowth flux and LUC emissions. Regrowth flux represents the post LUC effect on ecosystem CO_2 exchange (i.e., NEP); thus, it was extracted by subtracting NEP of the S2 from that of the S3 (NEP differs from NBP by excluding disturbance fluxes from fire and LUC). The rest of net LUC flux components (i.e., emissions from removed wood products) were defined as LUC emissions, which was estimated by subtracting regrowth flux from net LUC flux (Table 1).

2.2.3. Land use change forcing

The LUC forcing for the TRENDY models provides gridded information of land cover changes between cropland, pastureland, and primary and secondary lands, based on the U.N. Food and Agricultural Organization (FAO) national statistics. The initial land cover changes (annual transitions of cropland and pastureland at the spatial resolution of 5') were calculated using allocation algorithms and time-dependent weighting maps based on global historical population density, soil suitability, distance to rivers, lakes, slopes, and biome distributions (HistorY Database of the Global Environment: HYDE v3.1; Klein Goldewijk et al., 2011). The LUH v1, an extended version of HYDE, then combined the HYDE cropland and pastureland status with the wood harvest information from the FAO national statistics with an empirically estimated biomass density map produced at the spatial resolution of 0.5° (Hurtt et al., 2011). The LUH v1 provides the full annual transition matrix of primary and secondary lands in addition to those of cropland and pastureland.

The implementation of the LUC forcing was left to the discretion of each TRENDY modeling group because of differences in fundamental assumptions and levels of complexity in LUC modeling, for instance, distinction of primary and secondary lands, implementation of wood and crop harvests, consideration of residue carbon after deforestation, and turnover rates of a product pool (Table S1; more details shown in Le Quéré et al., 2015). Despite these differences in LUC schemes, land cover changes predefined by the LUC forcing data ensure relatively consistent forest area changes among the TRENDY models (minor differences occur, e.g. due to dynamic vegetation).

2.3. Independent estimates of net CO_2 flux

2.3.1. Atmospheric CO_2 inversions

Atmospheric CO_2 inversions estimate net land-atmosphere CO_2 flux from the continuous and discrete atmospheric CO_2 measurements from global networks, e.g., NOAA Earth System Research Laboratory (NOAA/ESRL: https://www.esrl.noaa.gov/gmd/ccgg/trends/full.html), World Data Centre for Greenhouse Gases (WDCGG: http://ds.data.jma.go.jp/gmd/wdcgg/wdcgg.html), and Comprehensive Observation Network for TRace gases by AIrLiner (CONTRAIL: http://www.cger.nies.go.jp/contrail/), and the prior fluxes (information on land and ocean fluxes, fire emissions, and anthropogenic CO_2 emissions). In this study, an ensemble of six atmospheric CO_2 inversions was used for validation of the biosphere models providing quasi-independent data for net CO_2 flux. Outputs of four inversions are from Thompson et al. (2016): ACTM v5.7b (Saeki & Patra, 2017), CCAM (Rayner et al., 2008), JMA-CDTM (Maki et al., 2010), and MACC v14r2 (Chevallier et al., 2010). Two others are from Peylin et al. (2013): JENA s81 v3.8 (Rödenbeck et al., 2003) and NICAM-TM (Niwa et al., 2012). A choice of CO_2 measurements and prior fluxes for each inversion system was left to the discretion of modeling groups, as well as spatial resolution and time period of inverted fluxes. Details of a transport model, prior fluxes, and CO_2 measurement data for these inversions are described in Thompson et al. (2016) and Peylin et al. (2013), and corresponding literature for each inversion. Using data from the six atmospheric CO_2 inversions, net CO_2 flux for the period 1980−2009 was estimated by an ensemble average for overlapping time periods (ACTM covers the period for 1990−2011; JENA and MACC for 1980−2014; CCAM for 1993−2012; JMA for 1985−2012; NICAM-TM for 1988−2007).

2.3.2. Residual method

The residual method from GCP (Le Quéré et al., 2015, 2016) provides the global annual budget of land CO_2 uptake calculated as the difference of the other terms of the global carbon budget such as the CO_2 growth rate (NOAA/ESRL), fossil fuel emissions from Carbon Dioxide Information Analysis Center (CDIAC: http://cdiac.ess-dive.lbl.gov/) and United Nations Framework Convention on Climate Change (UNFCCC: http://unfccc.int/ghg_data/items/3800.php), net ocean flux from ocean biogeochemistry models, and net LUC flux from the book-keeping model (Giglio et al., 2013; Houghton et al., 2012), i.e. land flux = CO_2 growth rate – fossil fuel emissions – ocean flux – net LUC flux. The land uptake calculated in the above-mentioned method does not account for the effect of LUC (that is provided by the land use change book-keeping model); thus, it represents an attribution from the CO_2 and climate effects on net CO_2 flux (broadly comparable to NBP of the TRENDY S2 simulations). Net CO_2 flux of GCP was estimated as a sum of the residual land uptake and net LUC flux from the book-keeping model, i.e., land flux + net LUC flux (comparable to the atmospheric CO_2 inversions and NBP from TRENDY S3 simulations). These land uptake estimates are referred to as GCP, hereafter.

2.4. Screening of biosphere models

In this study, we evaluate the relative contributions in terms of the difference between mean annual CO_2 fluxes for the 2000s and 1960s−1990s (termed ΔF), for the key components to net CO_2 flux (Table 1): climatological components (CO_2 fertilization effect, climate effect, and their net effect termed CO_2+climate effect) and LUC components (LUC emissions, regrowth flux, and their net flux termed net LUC flux). As ΔF is the key variable of the analysis, accurate simulations of CO_2 budgets for the 2000s and 1960s−1990s are required. Therefore, we examined the degree of agreement between the independent estimates of net CO_2 flux (GCP and atmospheric CO_2 inversions) and the eight biosphere models of TRENDY: the Community Land Model v4.5: CLM (Lawrence et al., 2011), Integrated Science Assessment Model: ISAM (Jain et al., 2013), Joint UK Land Environment Simulator v3.2: JULES (Clark et al., 2011), Lund-Potsdam-Jena DGVM wsl: LPJ (Sitch et al., 2003), LPJ-GUESS (Smith et al., 2001), LPX (Stocker et al., 2014), ORCHIDEE-CN: O-CN (Zaehle and Friend, 2010), and Vegetation Integrative SImulator for Trace gases: VISIT (Ito, 2010).

For the period 1960−2012, all the TRENDY models were relatively consistent in patterns of interannual variability (IAV) and trends of global net CO_2 flux with respect to the GCP and atmospheric CO_2 inversions, but for some the consistency was particularly notable (Fig. S1). To quantify the level of consistency, we examined a residual sum of squares (RSS) between the TRENDY models and GCP for the periods 1960−2012 and 2000−2012 (Fig. S2). Four models (CLM, JULES, O-CN, and VISIT) yielded a substantially lower RSS than the others for both time periods, and an ensemble of the four models resulted in highly consistent IAV in net CO_2 flux with respect to the GCP ($r = 0.70$, $p < 0.01$) and atmospheric CO_2 inversions ($r = 0.75$, $p < 0.01$) (Fig. S3).

We cross-checked mean annual CO_2 budgets (from S3 NBP and S2 NBP) for the 2000s and 1960s−1990s between the biosphere models with lower RSS and others (Fig. S4). Decadal CO_2 budgets by an ensemble of the four models with lower RSS were consistent with the GCP and atmospheric CO_2 inversions, whereas an ensemble of the other models yielded a weaker sink compared with the independent estimates. Based on these evaluations, we selected the four models, CLM, JULES, O-CN, and VISIT, for the following analysis.

3. Results

3.1. Increasing CO_2 uptake and contribution of regrowth flux

The biosphere models of this analysis (the four models evaluated against the GCP and atmospheric CO_2 inversions) support the recent increase in CO_2 uptake by the terrestrial biosphere (Fig. 1a). Decadal variability in global net CO_2 flux by the ensemble of the biosphere models (S3 NBP) indicates a tendency toward a net source during the 1910s−1950s and a transition toward a net sink during the 1960s−2000s (Fig. 1a and Fig. S5). The transition from a net source to a net sink in the 1960s is in line with that simulated by an Earth system model (Shevliakova et al., 2013). The increasing CO_2 uptake since the 1960s results in the 2000s displaying a larger decadal CO_2 uptake than at any time during the preceding century, -1.52±0.31 Pg C yr^{-1} (average ± 1σ as model-by-model variability).

We found that both climatological and LUC components ($\Delta F_{CO2+clim}$ and ΔF_{LUC}, respectively: Table 1) contributed to the recent enhancement of global CO_2 uptake (indicated by ΔF_{net}), which amounted to -1.27±0.34 Pg C yr^{-1} (Fig. 1b). Components of net CO_2 flux by the GCP agree with the pattern of relative contributions by the biosphere models (Fig. 1b; see Fig. S6 for individual biosphere model results). Examining the individual relative contributions further, we found that despite its large contribution, the CO_2 fertilization effect (ΔF_{CO2}) does not fully explain the recent enhancement in CO_2 uptake. A relative contribution from ΔF_{CO2} to $\Delta F_{net,}$ -1.11±0.25 Pg C yr^{-1}, is reduced to -0.92±0.29 Pg C yr^{-1} when combined with climate effect (ΔF_{clim}), which induced a shift towards a net source in the 2000s (Fig. 1b and S6). Importantly, the remainder of ΔF_{net} is accounted for by the net LUC flux (ΔF_{LUC}), -0.37±0.21 Pg C yr^{-1}, of which regrowth flux (ΔF_{reg}) is the primary constituent at -0.33±0.10 Pg C yr^{-1}. The pattern of the relative contribution from ΔF_{reg} is considered robust because the ratio of ΔF_{reg} to ΔF_{net} is consistent between the individual biosphere models with a range of 23−30% (Fig. 1c), and is accompanied by a consistent trend toward a net sink throughout the past 50 years (-0.01 Pg C yr^{-2}, $p < 0.01$ by Mann-Kendall test; Fig. 1d). As a result, regrowth flux appears to have mitigated the increasing trend of LUC emissions during the 1960s−1990s, and further facilitated the decreasing trend in LUC emissions during the 1990s−2000s (Fig. 1d).

3.2. Spatial pattern and hotspots of the uptake enhancement by plant regrowth

A closer look at regional patterns of the relative contributions reveals a clear distinction in locations responsible for the uptake enhancement between the climatological and LUC components. As illustrated in the spatial distribution of ΔF_{net}, the uptake enhancement has occurred over large proportions of vegetated area across the globe (Fig. 2a), but with substantial regional variations (the regional classification is shown in Fig. S7). The contribution from $\Delta F_{CO2+climate}$ was widespread from boreal Eurasia to tropical regions such as coastal regions of South America, central Africa, and tropical Asia (Fig. 2b). In contrast, the contribution from ΔF_{LUC} was concentrated in three particular regions: an eastern part of North America, southern and eastern parts of Europe (including European Russia), and a southeastern part of Temperate Eurasia (hereafter, hot-spots in ΔF_{LUC}: Fig. 2c). It is important to note that these hot-spots in ΔF_{LUC} largely coincide with locations where a large contribution from ΔF_{reg} is found (especially in North America and Europe; Fig. S8), and these patterns are consistent between the biosphere models (Figs. S9 and S10). The three regions characterized by large ΔF_{reg} accounted for 94% of the global total (Table S2), with the largest contribution from North America (-0.17±0.03 Pg C yr^{-1}). In North America, we found that a large fraction of ΔF_{CO2} (-0.21±0.04 Pg C yr^{-1}) was cancelled by $\Delta F_{climate}$ (0.13±0.08 Pg C yr^{-1}), which clearly demonstrates that the enhanced uptake indicated by ΔF_{net} (-0.24±0.06 Pg C yr^{-1}) cannot be explained without the contribution from regrowth flux during the 2000s (Table S2).

Focusing on the hot-spots in ΔF_{LUC} (colored grid cells in Figure 3), we found that IAVs in net LUC flux and NEP in the North American and European hot-spots have a similar tendency toward a net sink for the past 50 years when the effect of land use and land over changes is taken into account for NEP, i.e. S3 NEP (Fig. 3a, b). Zonally-averaged fluxes indicate that the shift from a net source to net sink in net LUC flux between the 1960s and 2000s in Europe and North America corresponds closely to the emergence of a strong regrowth sink in those locations over this time (Fig. 3d, e). Contrary to North America and Europe, the hot-spot in temperate Eurasia indicates a relatively less uptake from regrowth flux during the 2000s (Fig. 3c, 3f), suggesting that a decrease in LUC emissions is the factor also responsible for the change in net LUC flux (Fig. S8c, d).

4. Discussion and conclusions

Our approach for attribution of the net CO_2 flux revealed that both regrowth after LUC and growth enhancement due to CO_2 fertilization are responsible for the recent enhancement of CO_2 uptake, but the quantification of these effects still presents potential large uncertainties. A recent synthesis of biosphere models argues that LUC emissions may previously have been underestimated, due to the neglect, until very recently, of processes such as shifting cultivation, wood harvest and cropland management (Arneth et al., 2017). Arneth et al. (2017) suggests that such an underestimation implies a larger land CO_2 uptake than previously thought. Because of a large contribution to the net CO_2 balance (Fig. 1), the CO_2 fertilization may be a strong candidate for this additional CO_2 uptake. However, physiological evidences from long-term inventory (Clark et al., 2010) and carbon isotope measurements (van der Sleen et al., 2015) criticize a strong CO_2 fertilization effect in tropics, posing a question on its dominate role in the recent uptake enhancement.

Local studies support reliability of the hot-spots of plant regrowth found in this study. Regional analyses of extensive forest inventory measurements have reported that a large fraction of the current forest carbon stock accumulations in the eastern part of North America (specifically, the eastern US) and European countries originates from the large-scale reforestation and afforestation during the post-war period in the 1960s (Pacala et al., 2001; Ciais et al., 2008; Woodall et al., 2015). The LUC forcing used for the biosphere models reflects these regional characteristics, indicating a decadal land conversion with a substantial increase in secondary forests and the corresponding decrease in cropland between 1960 and 2000 (Figs. S11 and S12). This corroboration of historical LUC increases a confidence in the modeled increase in CO_2 uptake due to plant regrowth during recent years, and the likely continuation of forest conservation in US and European countries (Forest Europe, 2015; USDA Forest Service, 2016) suggests a further increase in CO_2 uptake by plant regrowth in the future.

In addition to plant regrowth, the decrease in LUC emissions also contributed to the change in net LUC flux in temperate Eurasia. However, this causality should be interpreted with caution. Large-scale afforestation programs have been initiated in eastern China since the 1980s, which led to an increase in forest area at 1.6 % per year over the 1990s−2000s (Piao et al., 2012; Peng et al., 2014). Nevertheless, the LUC forcing for the biosphere models does not indicate any notable increase in secondary forests during the past 50 years in this region, instead a large fraction of primary forests is replaced by croplands and pastures (Figs. S11 and S12). This mismatch between the real event and LUC forcing in temperate Eurasia might have caused an underestimation of CO_2 uptake in the absence of regrowth of secondary forests, and it calls for an immediate improvement of the LUC forcing for this region.

Although the biogeochemical effects of plant regrowth from historical land use and management has likely moderated rates of present day climate change, the biophysical effect of land cover changes may act in the opposite direction, especially on the local-regional scale (Alkama and Cescatti, 2016). For example, in Europe, continuous afforestation from past has led to an increase in land CO_2 uptake, but species change from broadleaf to needleleaf forests resulted in a regional increase of the summertime temperature because of a decrease in evapotranspiration (Naudts et al., 2016). Thus, the net effect of plant regrowth on climate is complex and scale-dependent, and further work is required integrating over both biogeochemical and biophysical effects of plant regrowth at both regional and global scales. This will require complementing the existing datasets that identify wood harvest and transitions between forests, croplands, and pastures, with estimates of forest age, and tree species changes due to management.

Acknowledgements

M. K., K. I., and P. K. P. acknowledge Environment Research and Technology Development Funds of the Ministry of the Environment of Japan (2-1401) and of the Environmental Restoration and Conservation Agency (2-1701). T.A.M.P. acknowledges funding from European Commission’s Seventh

Framework Programme, under grant agreement number 603542 (LUC4C). L.C. acknowledges support from the National Aeronautics and Space Administration Earth and Space Science Fellowship, under grant number NNX16AP86H. The TRENDY data are available via Dr. Stephen Sitch, Exeter University (s.a.sitch@exeter.ac.uk). MACC and JENA inversion data are available from the web sites (MACC: http://apps.ecmwf.int/datasets/data/macc-ghg-inversions/, JENA: http://www.bgc-jena.mpg.de/CarboScope/s/main.html). ACTM, JMA, and CCAM inversion data used in this study are from Asia-Pacific Network for Global Change Research (APN: grant#ARCP2011-11NMY-Patra/Canadell) and available by contacting Dr. Prabir K. Patra (prabir@jamstec.go.jp). NICAM inversion data are available by contacting Dr.Yosuke Niwa (niwa.yosuke@nies.go.jp or yniwa@mri-jma.go.jp). Flux data of Global Carbon Project are available from the web site (http://cdiac.ess-dive.lbl.gov/GCP/).

References

Alkama, R. and Cescatti, A. (2016). Biophysical climate impacts of recent changes in global forest cover. Science, 351, 600-604.

Arneth, A., Sitch, S., Pongratz, J., Stocker, B. D., Ciais, P., Poulter, B., ... Zaehle, S. (2017). Historical carbon dioxide emissions caused by land-use changes are possibly larger than assumed. Nature Geoscience, 10, 79–84.

Arora, V. K. and Scinocca, J. F. (2016). Constraining the strength of the terrestrial CO_2 fertilization effect in the Canadian Earth system model version 4.2 (CanESM4.2). Geoscientific Model Development, 9, 2357-2376.

Ballantyne, A. P., Alden, C. B., Miller, J. B., Tans, P. P., and White, J. W. C. (2012). Increase in observed net carbon dioxide uptake by land and oceans during the past 50 years. Nature, 488, 70–72.

Ballantyne, A. P., Smith, W., Anderegg, W., Kauppi, P., Sarmiento, J., Tans, P., … Running, S. (2017). Accelerating net terrestrial carbon uptake during the warming hiatus due to reduced respiration. Nature Climate Change, 7, 148–152.

Chapin, F. S., Woodwell, G. M., Randerson, J. T., Rastetter, E. B., Lovett, G. M., Baldocchi, D. D., ... Schulze, E.-D. (2006). Reconciling carbon-cycle concepts, terminology, and methods. Ecosystems, 9, 1041–1050.

Chevallier, F., Ciais, P., Conway, T. J., Aalto, T., Anderson, B. E., Bousquet, P., ... Worthy, D. (2010). CO_2 surface fluxes at grid point scale estimated from a global 21 year reanalysis of atmospheric measurements. Journal of Geophysical Research, 115, D21307.

Ciais, P., Schelhaas, M. J., Zaehle, S., Piao, S. L., Cescatti, A., Liski, J., ... Nabuurs, G. J. (2008). Carbon accumulation in European forests. Nature Geoscience, 1, 425-429.

Clark, D. B., Mercado, L. M., Sitch, S., Jones, C. D., Gedney, N., Best, M. J., ... Cox, P. M. (2011). The Joint UK Land Environment Simulator (JULES), model description – Part 2: carbon fluxes and vegetation dynamics. Geoscientific Model Development, 4, 701–722.

Clark, D. B., Clark, D. A. and Oberbauer, S. F. (2010). Annual wood production in a tropical rain forest in NE Costa Rica linked to climatic variation but not to increasing CO_2. Global Change Biology, 16, 747–759.

Cox, P. M., Pearson, D., Booth, B. B., Friedlingstein, P., Huntingford, C., Jones, C. D., and Luke, C. M. (2013). Sensitivity of tropical carbon to climate change constrained by carbon dioxide variability. Nature, 494, 341–344.

DeVries, T., Holzer, M., and Primeau, F. (2017). Recent increase in oceanic carbon uptake driven by weaker upper-ocean overturning. Nature, 542, 215–218.

Erb, K.-H., Kastner, T., Luyssaert, S., Houghton, R. A., Kuemmerle, T., Olofsson, P., and Haberl, H. (2013). Bias in the attribution of forest carbon sinks. Nature Climate Change, 3, 854–856.

Erb, K.-H., Kastner, T., Plutzar, C., Bais, A. L. S., Carvalhais, N., Fetzel, T., ... Luyssaert, S. (2018).Unexpectedly large impact of forest management and grazing on global vegetation biomass. Nature, 553, 73–76.

Fisher, J. B., Sikka, M., Sitch, S., Ciais, P., Poulter, B., Galbraith, D., ... Malhi, Y. (2013). African tropical rainforest net carbon dioxide fluxes in the twentieth century. Philosophical Transactions of the Royal Society B, 368, 20120376.

Forest Europe (2015). State of Europe's forests 2015, edited by Ministerial Conference on the Protection of Forests in Europe, FOREST EUROPE Liaison Unit Madrid, Spain (2015).

Fyfe, J. C., Meehl, G. A., England, M. H., Mann, M. E., Santer, B. D., Flato, G. M., ... Swart, N. C. (2016). Making sense of the early-2000s warming slowdown. Nature Climate Change, 6, 224–228.

Giglio, L., Randerson, J., and van der Werf, G. (2013). Analysis of daily, monthly, and annual burned area using the fourth-generation global fire emissions database (GFED4). Journal of Geophysical Research – Biogeosciences, 118, 317–328.

Harris, I., Jones, P. D., Osborn, T. J. and Lister, D. H. (2014). Updated high-resolution grids of monthly climatic observations – the CRU TS3.10 Dataset. International Journal of Climatology, 34, 623–642.

Houghton, R. A., and Nassikas, A. A. (2017). Global and regional fluxes of carbon from land use and land cover change 1850–2015. Global Biogeochemical Cycles, 31, 456–472.

Houghton, R. A., House, J. I., Pongratz, J., van der Werf, G. R., DeFries, R. S., Hansen, M. C., Le Quéré, C., and Ramankutty, N. (2012). Carbon emissions from land use and land-cover change. Biogeosciences, 9, 5125-5142.

Hurtt, G. C., Chini, L. P., Frolking, S., Betts, R. A., Feddema, J., Fischer, G., ... Wang, Y. P. (2011). Harmonization of land-use scenarios for the period 1500–2100: 600 years of global gridded annual land-use transitions, wood harvest, and resulting secondary lands. Climatic Change, 109, 117–161.

Ito, A. (2010). Evaluation of the impacts of defoliation by tropical cyclones on a Japanese forest's carbon budget using flux data and a process-based model. Journal of Geophysical Research, 115, G04013.

Jain, A. K., Meiyappan, P., Song, Y. and House, J. I. (2013). CO_2 emissions from land-use change affected more by nitrogen cycle, than by the choice of land-cover data. Global Change Biology, 19, 2893–2906.

Keeling, R. F., Graven, H. D., Welp, L. R., Resplandy, L., Bi, J., Piper, S. C., ... Meijer, H. A. J. (2017). Atmospheric evidence for a global secular increase in carbon isotopic discrimination of land photosynthesis. Proceedings of the National Academy of Sciences USA, 114, 10361–10366.

Keenan, T. F., Prentice, I. C., Canadell, J. G., Williams, C. A , Wang, H., Raupach, M., and Collatz, G. J. (2016). Recent pause in the growth rate of atmospheric CO_2 due to enhanced terrestrial carbon uptake. Nature Communications, 7, 13428.

Kistler, R., Collins, W., Saha, S., White, G., Woollen, J., Kalnay, E., ... Fiorino, M. (2001). The NCEP–NCAR 50-year reanalysis: monthly means CD–ROM and documentation. Bulletin of the American Meteorological Society, 82, 247–267.

Klein Goldewijk, K., Beusen, A., van Drecht, G. and de Vos, M. (2011). The HYDE 3.1 spatially explicit database of human-induced global land-use change over the past 12,000 years. Global Ecology and Biogeography, 20, 73–86.

Lawrence, D. M., Oleson, K. W., Flanner, M. G., Thornton, P. E., Swenson, S. C., Lawrence, P. J., ... Slater, A. G. (2011). Parameterization improvements and functional and structural advances in version 4 of the community land model. Journal of Advances in Modeling Earth Systems, 3, M03001.

Le Quéré, C., Andrew, R. M., Canadell, J. G., Sitch, S., Korsbakken, J. I., Peters, G. P., ... Zaehle, S. (2016). Global Carbon Budget 2016. Earth System Science Data, 8, 605-649.

Le Quéré, C., Moriarty, R., Andrew, R. M., Canadell, J. G., Sitch, S., Korsbakken, J. I., ... Zeng, N. (2015). Global Carbon Budget 2015, Earth System Science Data, 7, 349-396.

Maki, T., Ikegami, M., Fujita, T., Hirahara, T., Yamada, K., Mori, K., ... Conway, T. J. (2010). New technique to analyze global distributions of CO_2 concentrations and fluxes from non-processed observational data. Tellus B, 62, 797–809.

Naudts, K., Chen, Y., McGrath, M. J., Ryder, J., Valade, A., Otto, J., Luyssaert, S. (2016). Europe's forest management did not mitigate climate warming. Science, 351, 597-600.

Niwa, Y., Machida, T., Sawa, Y., Matsueda, H., Schuck, T. J., Brenninkmeijer, C. A. M., ... Satoh, M. (2012). Imposing strong constraints on tropical terrestrial CO_2 fluxes using passenger aircraft based measurements. Journal of Geophysical Research, 117, D11303.

Pacala, S. W., Hurtt, G. C., Baker, D., Peylin, P., Houghton, R. A., Birdsey, R. A., ... Field, C. B. (2001). Consistent Land- and Atmosphere-Based U.S. Carbon Sink Estimates. Science, 292, 2316-2320.

Pan, Y., Birdsey, R. A., Fang, J., Houghton, R., Kauppi, P. E., Kurz, W. A., ... Hayes, D. (2011). A large and persistent carbon sink in the world's forests. Science, 333, 988–993.

Peng, S.-S., Piao, S. L., Zeng, Z., Ciais, P., Zhou, L., Li, L. Z. X., ... Zeng, H. (2014). Afforestation in China cools local land surface temperature. Proceedings of the National Academy of Sciences USA, 111, 2915–2919.

Peylin, P., Law, R. M., Gurney, K. R., Chevallier, F., Jacobson, A. R., Maki, T., ... Zhang, X. (2013). Global atmospheric carbon budget: results from an ensemble of atmospheric CO_2 inversions, Biogeosciences, 10, 6699-6720.

Piao, S. L., Ito, A., Li, S. G., Huang, Y., Ciais, P., Wang, X. H., ... Zhu, B. (2012). The carbon budget of terrestrial ecosystems in East Asia over the last two decades. Biogeosciences 9, 3571-3586.

Rödenbeck, C., Houweling, S., Gloor, M., and Heimann, M. (2003). CO_2 flux history 1982-2001 inferred from atmospheric data using a global inversion of atmospheric transport. Atmospheric Chemistry and Physics, 3, 1919–1964.

Sarmiento, J. L., Gloor, M., Gruber, N., Beaulieu, C., Jacobson, A. R., Mikaloff Fletcher, S. E., Pacala, S., and Rodgers, K. (2010). Trends and regional distributions of land and ocean carbon sinks. Biogeosciences, 7, 2351-2367.

Schimel, D., Stephens, B. B., and Fisher, J. B. (2015). Effect of increasing CO_2 on the terrestrial carbon cycle. Proceedings of the National Academy of Sciences USA, 112, 436–441.

Shevliakova, E., Stouffer, R. J., Malyshev, S., Krasting, J. P., Hurtt, G. C., and Pacala, S. W. (2013). Historical warming reduced due to enhanced land carbon uptake. Proceedings of the National Academy of Sciences USA, 110, 16730–16735.

Sitch, S., Smith, B., Prentice, I. C., Arneth, A., Bondeau, A., Cramer, W., ... and Venevsky, S. (2003). Evaluation of ecosystem dynamics, plant geography and terrestrial carbon cycling in the LPJ dynamic vegetation model. Global Change Biology, 9, 161–185.

Sitch, S., Friedlingstein, P., Gruber, N., Jones, S. D., Murray-Tortarolo, G., Ahlström, A., ... Myneni, R. (2015). Recent trends and drivers of regional sources and sinks of carbon dioxide. Biogeosciences, 12, 653-679.

Smith, B., Prentice, I. C., and Sykes, M. T. (2001). Representation of vegetation dynamics in the modelling of terrestrial ecosystems: comparing two contrasting approaches within European climate space. Global Ecology and Biogeography, 10, 621–637.

Stocker, B. D., Spahni, R., and Joos, F. (2014). A cost efficient TOPMODEL implementation to simulate sub-grid spatio-temporal dynamics of global wetlands and peatlands. Geoscientific Model Development, 7, 3089–3110.

Sun, Y., Gu, L., Dickinson, R. E., Norby, R. J., Pallardy, S. G., and Hoffman, F. M. (2014) Impact of mesophyll diffusion on estimated global land CO_2 fertilization, Proceedings of the National Academy of Sciences USA, 111, 15774–15779.

Thompson, R. L., Patra, P. K., Chevallier, F., Maksyutov, S., Law, R. M., Ziehn, T., ... Ciais, P. (2016). Top–down assessment of the Asian carbon budget since the mid 1990s. Nature Communications, 7, 19724.

USDA Forest Service (2016). Future of America's Forests and Rangelands: Update to the 2010 Resources Planning Act Assessment, General Technical Report, WO-GTR-94, Washington DC.

van der Sleen, P., Groenendijk, P., Vlam, M., Anten, N. P. R., Boom, A., Bongers, F., ... Zuidema, P. A. (2015). No growth stimulation of tropical trees by 150 years of CO_2 fertilization but water-use efficiency increased. Nature Geoscience, 8, 24–28.

Wang, W., Ciais, P., Nemani, R. R., Canadell, J. G., Piao, S. L., Sitch, S., ... Myneni, R. B. (2013). Variations in atmospheric CO_2 growth rates coupled with tropical temperature. Proceedings of the National Academy of Sciences USA, 110, 13061–13066.

Woodall, C. W., Walters, B. F., Coulston, J. W., D'Amato, A. W., Domke, G. M., Russell, M. B., and Sowers, P. A. (2015). Monitoring Network Confirms Land Use Change is a Substantial Component of the Forest Carbon Sink in the eastern United States. Scientific Reports, 5, 17028.

Zaehle, S. and Friend, A. D. (2010). Carbon and nitrogen cycle dynamics in the O-CN land surface model, I: Model description, site-scale evaluation and sensitivity to parameter estimates. Global Biogeochemical Cycles, 24, GB1005.

Zhao, F., Zeng, N., Asrar, G., Friedlingstein, P., Ito, A., Jain, A., ... Zaehle, S. (2016). Role of CO_2, climate and land use in regulating the seasonal amplitude increase of carbon fluxes in terrestrial ecosystems: a multimodel analysis. Biogeosciences, 13, 5121-5137.

Zhu, Z., Piao, S. L., Myneni, R. B., Huang, M., Zeng, Z., Canadell, J. G., ... Zeng, N. (2016). Greening of the Earth and its drivers. Nature Climate Change, 6, 791–795.

Table 1. Descriptions of flux terminologies and calculation methods.

Terminology	Calculation method[*†]	Description	Symbol for ΔF
Net CO_2 flux (**1+2**)	S3 NBP	Net exchange of CO_2 uptake and release between land and atmosphere, accounting the spatio-temporal variability in historical CO_2, climate, and LUC.	ΔF_{net}
1. CO_2+climate effect (**1a+1b**)	S2 NBP	Partial net exchange of CO_2 accounting for spatio-temporal variability in historical CO_2, and climate.	$\Delta F_{CO2+climate}$
1a. CO_2 effect	S1 NBP	Partial net exchange of CO_2 accounting for spatio-temporal variability in historical CO_2 only.	ΔF_{CO2}
1b. Climate effect	S2 NBP – S1 NBP	Partial net exchange of CO_2 accounting for spatio-temporal variability in historical climate only.	$\Delta F_{climate}$
2. Net LUC flux (**2a+2b**)	S3 NBP – S2 NBP	Partial net exchange of CO_2 accounting for spatio-temporal variability in historical LUC only. This flux constitutes of CO_2 uptake and release by LUC and plant regrowth.	ΔF_{LUC}
2a. LUC emissions	(S3 NBP – S2 NBP) – (S3 NEP – S2 NEP)	CO_2 emissions from wood storages removed by LUC. It is the dominant component of gross LUC source.	ΔF_{LUCe}
2b. Regrowth flux	S3 NEP – S2 NEP	Exchange of CO_2 uptake and release during the process of plant regrowth after LUC. This flux is the dominant component of gross LUC sink, but it also includes emissions from decomposition of woody residues (i.e., litters) remaining on sites.	ΔF_{reg}

*NBP: Net Biome Production (photosynthesis - autotrophic and heterotrophic respirations - natural disturbances - LUC emissions), NEP: Net Ecosystem Productivity (photosynthesis - autotrophic and heterotrophic respirations)

†S3: simulation forced with varying CO_2, climate, and LUC, S2: simulation forced with varying CO_2 and climate, and S1: simulation forced with varying CO_2.

Figure 1. Increasing pattern of global CO_2 uptake and contributions of component fluxes.

a, Decadal variability of global net CO_2 flux from the ensemble mean of the four TRENDY models: (S3 NBP: orange) for the 1910s−2000s, Global Carbon Project (GCP: grey) for the 1960s−2000s, and the ensemble mean of the atmospheric CO_2 inversions (cyan) for the 1980s−2000s. Negative values in net CO_2 flux represent a net sink, and positive values a net source. Error bars indicate 1σ variations among models. A top-right panel shows correlation coefficients (*r*) between interannual variability of the three net CO_2 flux estimates for the overlapping periods (1980−2009 for the TRENDY and atmospheric CO_2 inversions; 1960−2009 for the TRENDY and GCP, and 1980−2009 for the atmospheric CO_2 inversions and GCP) and statistical significance is indicated by ** ($p < 0.01$). A middle panel shows mean annual CO_2 budgets of attributing factors to net CO_2 flux (CO_2 effect, climate effect, and net LUC flux) for the periods 1910−1959 and 1960−2009. **b,** Changes of global CO_2 uptake in the 2000s with respect to that during the 1960s−1999s (indicated by ΔF: difference between mean annual CO_2 budget for 2000−2009 and that for 1960−1999). ΔF for net CO_2 flux and component fluxes (refer to Table 1 for descriptions of component fluxes) by the TRENDY models (orange bars and coloured lines) are showed along with estimates by the GCP (grey bars). Negative values in ΔF represent that CO_2 flux in the 2000s is more toward a net sink than that in the 1960s−1990s, and positive values indicate the opposite. **c,** ΔF for net CO_2 flux (open bars) and regrowth flux (green bars) from the individual TRENDY models (CLM, JULES, O-CN, and VISIT) and their ensemble mean. **d,** Interannual variability of net LUC flux (red line), LUC emissions (purple line), and regrowth flux (green line) by the TRENDY models in the form of anomaly with a base period 1960−2009. For each flux, shading indicates 1σ variations among models. Dashed lines are linear regressions on the data for 1960−1999 and 1990−2009 and statistical significance is determined by Mann-Kendall test and indicated by ** ($p < 0.01$).

Figure 2. Spatial patterns of ΔF for net CO_2 flux and component fluxes.

Spatial variability in ΔF for **a,** net CO_2 flux (ΔF_{net}), **b,** CO_2+climate effect ($\Delta F_{CO2+climate}$), and **c,** net LUC flux (ΔF_{LUC}) by the ensemble mean of the TRENDY models. Along with spatial maps, regional budgets of ΔF based on the RECCAP land classification (Figure S7) are shown for net CO_2 flux, CO_2 and climate effects (ΔF_{CO2} and $\Delta F_{climate}$, respectively), regrowth flux (ΔF_{reg}), and LUC emissions (ΔF_{LUCe}). Negative values in ΔF represent that CO_2 flux in the 2000s is more toward a net sink than that in the 1960s−1990s, and positive values indicate the opposite.

Figure 3. Temporal transition of regrowth flux in the three hop-spot regions of ΔF_{LUC}.

Temporal variability (five-year averaged) of net LUC flux (red bar) and NEP with and without considering variability in LUC (green and grey lines, respectively) for the three hot-spot regions of ΔF_{LUC}, **a,** North America, **b,** Europe, and **c,** Temperate Eurasia. Error bars and shading indicate 1σ variations among models. A spatial map in background is from Figure 2c and the three regional hot-spots characterized by large negative ΔF_{LUC} are highlighted with different colours. Decadal changes in longitudinal averaged net LUC flux (red gradient lines) and regrowth flux (green gradient lines) over the three hot-spot regions, **d,** North America, **e,** Europe, and **f,** Temperate Eurasia. All results are from the TRENDY models.

Figure 1.

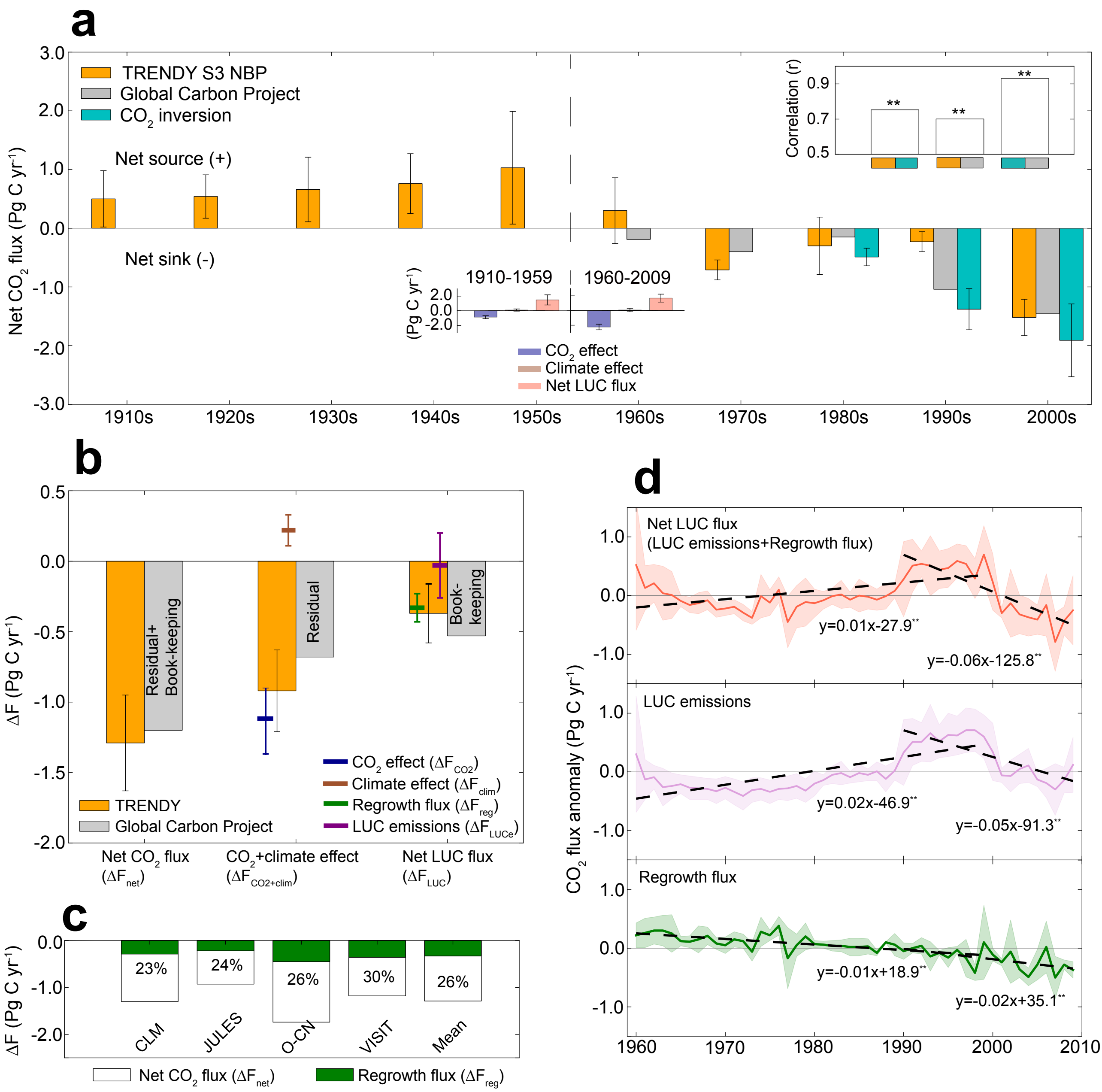

a
TRENDY S3 NBP
Global Carbon Project
CO2 inversion
Net source (+)
Net sink (-)
Net CO2 flux (Pg C yr-1)
Correlation (r)
**
1910-1959
1960-2009
(Pg C yr-1)
CO2 effect
Climate effect
Net LUC flux
1910s
1920s
1930s
1940s
1950s
1960s
1970s
1980s
1990s
2000s
b
ΔF (Pg C yr-1)
Residual+ Book-keeping
Residual
Book-keeping
CO2 effect (ΔFCO2)
Climate effect (ΔFclim)
Regrowth flux (ΔFreg)
LUC emissions (ΔFLUCe)
TRENDY
Global Carbon Project
Net CO2 flux (ΔFnet)
CO2+climate effect (ΔFCO2+clim)
Net LUC flux (ΔFLUC)
c
ΔF (Pg C yr-1)
23%
24%
26%
30%
26%
CLM
JULES
O-CN
VISIT
Mean
Net CO2 flux (ΔFnet)
Regrowth flux (ΔFreg)
d
Net LUC flux
(LUC emissions+Regrowth flux)
y=0.01x-27.9**
y=-0.06x-125.8**
LUC emissions
y=0.02x-46.9**
y=-0.05x-91.3**
Regrowth flux
y=-0.01x+18.9**
y=-0.02x+35.1**
CO2 flux anomaly (Pg C yr-1)

Figure 2.

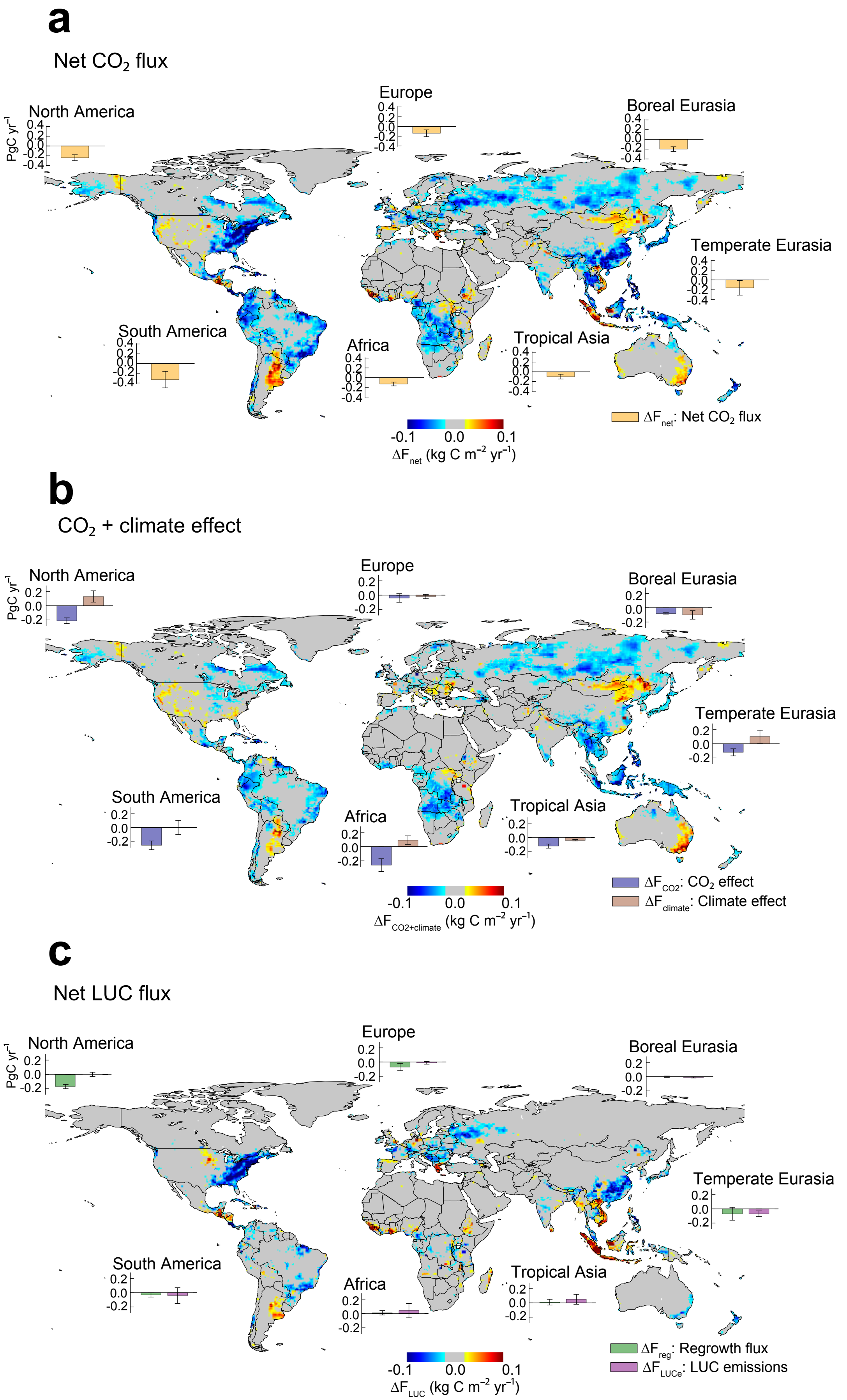

a
Net CO2 flux
North America
Europe
Boreal Eurasia
Temperate Eurasia
South America
Africa
Tropical Asia
PgC yr-1
0.4
0.2
0.0
-0.2
-0.4
ΔFnet: Net CO2 flux
-0.1
0.0
0.1
ΔFnet (kg C m-2 yr-1)
b
CO2 + climate effect
North America
Europe
Boreal Eurasia
Temperate Eurasia
South America
Africa
Tropical Asia
PgC yr-1
0.2
0.0
-0.2
ΔFCO2: CO2 effect
ΔFclimate: Climate effect
-0.1
0.0
0.1
ΔFCO2+climate (kg C m-2 yr-1)
c
Net LUC flux
North America
Europe
Boreal Eurasia
Temperate Eurasia
South America
Africa
Tropical Asia
PgC yr-1
0.2
0.0
-0.2
ΔFreg: Regrowth flux
ΔFLUCe: LUC emissions
-0.1
0.0
0.1
ΔFLUC (kg C m-2 yr-1)

Figure 3.

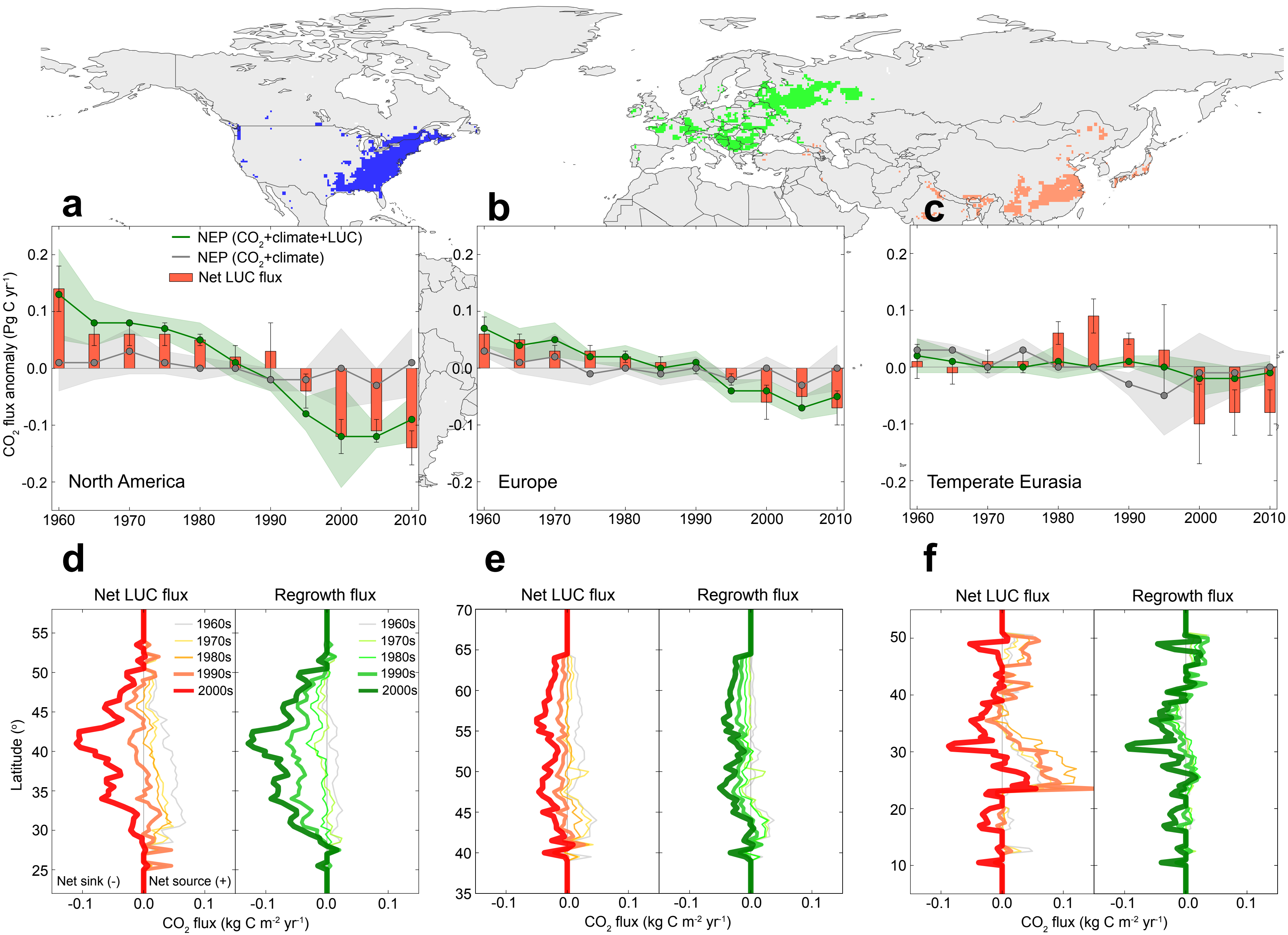
a
b
c
NEP (CO2+climate+LUC)
NEP (CO2+climate)
Net LUC flux
CO2 flux anomaly (Pg C yr-1)
North America
Europe
Temperate Eurasia
d
e
f
Net LUC flux
Regrowth flux
1960s
1970s
1980s
1990s
2000s
Latitude (°)
Net sink (-)
Net source (+)
CO2 flux (kg C m-2 yr-1)